Final Report

Project Title: Analysis of New Spectral Constraints on Jupiter's Cloud Structure

Award Number: NNX09AE07G

UW Account Number: PRJ23YA

For the Period of: 05/01/2009 – 04/30/2014

Principal Investigator: Lawrence A. Sromovsky

Location: University of Wisconsin – Madison
Space Science and Engineering Center
1225 West Dayton Street
Madison, WI 53707

Reports will be sent to:
Grants Officer
NASA Shared Services Center
Procurement Office, Bldg 1111
Stennis Space Center, MS 39529
NSSC-Grant-Report@mail.nasa.gov

Technical Officer
Attn: Max Bernstein
NASA Headquarters
Mail Code: 3K39
300 E Street SW, Suite
Washington, DC 20546
max.bernstein@nasa.gov

New Technology Office
Attn : New Technology Representative
NASA Goddard Space Flight Center
Greenbelt, MD 20771
Dale.L.Clarke@nasa.gov

Final Report submission to:
NSSC-closeout@mail.nasa.gov

(To be completed by the Principal Investigator)

Inventions Report:
No inventions resulted from this grant.

Inventory Report:
No federally owned equipment is in the custody of the PI.

Publications:

Peer Reviewed Publications:

[1] Sromovsky, L.A., and P.M. Fry 2010. The source of 3-micron absorption in Jupiter's clouds: a reanalysis of ISO observations with new NH3 absorption models. *Icarus* **210**, 211-229.

[2] Sromovsky, L.A., and P.M. Fry, 2010. The source of 3-micron absorption in Jupiter's clouds: constraints from 2000 VIMS observations. *Icarus* **210**, 230-257.

[3] Sromovsky, L.A., and P.M. Fry, V. Boudon, A. Campargue, and A. Nikitin 2011. Near-IR methane absorption in outer planet atmospheres: comparison of line-by-line and band models. *Icarus* **218**, 1-23. (Partially supported by a Planetary Atmospheres Grant.)

[4] Li, Liming, K. H. Baines, M. A. Smith, R. A. West, S. Perez-Hoyos, H. J. Trammell, A. A. Simon Miller, B. J. Conrath, P. J. Gierasch, G. S. Orton, C. A. Nixon, G. Filacchione, **P. M. Fry**, and T. Momary. (2012), Emitted power of Jupiter based on Cassini CIRS and VIMS observations, J. Geophys. Res., 117, E11002.

[5]Sromovsky, L.A. and P.M. Fry 2014. Quantitative analysis of fresh ammonia ice clouds on Jupiter. Icarus, in preparation.

Abstracts/Conference Presentations:

[6] Sromovsky, L.A. and P.M. Fry. 2009. Evidence for widely distributed ammonia ice on Jupiter. *Bull. Am. Astron. Soc.* **41**, 1006.

[7] Sromovsky, L.A. and P.M. Fry. 2010. Evidence for NH_4SH as the primary 3-micron absorber in Jupiter's Clouds. *Bull. Am. Astron. Soc.* **42**, 1010.

[8] Sromovsky, L.A. and P. M. Fry. 2011. Comparison of line-by-line and band-model calculations of methane absorption in outer-planet atmospheres. Presented at the EPSC-DPS Joint Meeting in Nantes, France (43rd DPS meeting).

Summary of Technical Effort:

OBJECTIVES: We aimed to develop improved models of Jovian cloud structure using a combination of imaging and spectral observations acquired during the New Horizons 2007 flyby of Jupiter, and complementary data provided by Galileo and Cassini imaging and spectral observations acquired during the Cassini flyby of Jupiter at the end of 2000. The main New Horizons instrument of interest to this investigation is named Ralph, and includes a visible and near-IR multi-spectral imager (MVIC) and a near-IR Linear Etalon

Imaging Spectral Array (LEISA). The latter is analogous to the Cassini VIMS and Galileo NIMS instrument but covers the 1.25-2.5 micron spectral range, compared to 0.3-5 microns for VIMS and 0.7-5.2 microns for the Galileo NIMS. LEISA's great advantage is the vastly better spatial resolution, with sub-spacecraft resolution ranging from 137 km/pixel at 32.44 RJ to 350 km at 82.3 RJ. VIMS best at Jupiter was 4900 km. Thus these data provide complementary spectral ranges, spatial coverages, and spatial resolutions. Variations in methane, ammonia, and collision-induced absorption with wavelength will be used to probe the vertical structure of clouds; we also planned to use high-resolution observations to infer vertical location from the ratio of spatial variations in cloud reflectivity at wavelengths with different penetration depths.

TASKS: (1) Image and Spectral Data Processing; (2) Characterization of spectral types, (3) Inversion of cloud structure from near-IR spectra, (4) Characterization of differences between New Horizons and Cassini Epochs, and (5) Combined analysis of CCD imagery and spectra.

PROGRESS DURING YEAR 1:

We concentrated first on the problem of inversion of cloud structure from near-IR spectra (Task 3). We first needed to find an improved characterization of ammonia gas absorption. We compared new laboratory measurements by Bowles et al. (2008, Icarus 196, 612-624) with HITRAN 2004 (2008 has same ammonia lines), HITRAN 1996 (used by Brooke et al. 1998), and with VIMS observations via model calculations. Fig. 1 compares two-way ammonia transmissions to the 722-mb level in a clear atmosphere.
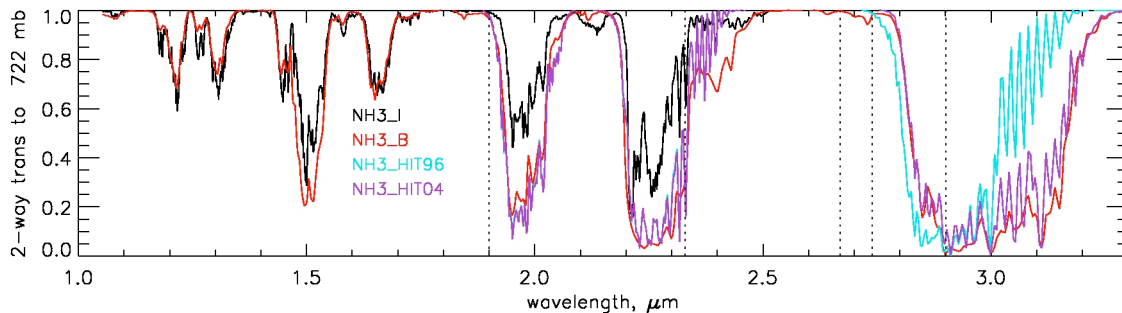
Figure 1. Spectral transmission due to different models of ammonia absorption. Here NH3_I refers to the earlier Irwin et al. (1999, JQSRT 62, 193-204) model, which stopped at 2.5 microns, NH3_B refers to the new Bowles band model, and HIT96 and HIT04 refer to the HITRAN models from 1996 and 2004 respectively.

We found that the Goody-Lorentz model of Bowles et al. was the best choice in most spectral regions, but where line-by-line calculations matched the G-L model under lab conditions, we decided to use the LBL results for Jovian conditions because of its better accounting for temperature dependence, foreign broadening, and pressure dependence. One peculiar result we found is that HITRAN96 has more lines in the 2.74-2.9 micron region than HITRAN04 and provides a better match to observed spectra than the GL model in that region as well. We thus found that a composite of sources provided the best overall absorption model. We fit the band and LBL models to ten-term exponential sum models (aka correlated-k). We also revised our opacity calculations to combine

3

NH3 and CH4 absorption more efficiently in regions where they are both important (reducing 10x10 terms to just 10 terms).

The second effort related to Task 3 was to implement the Levenberg-Marquardt algorithm for non-linear least-squares inversion. This enabled us to derive cloud structure parameters from spectra with an efficiency that provided enormous reductions in computation time, especially when one accounts for the fact that the algorithm yields parameter uncertainties at the same speed as the solutions. This enabled us to explore the implications of the widespread 3-micron absorption feature, which Brooke et al.(Icarus 136, 1-13, 1998) had interpreted to be due to ammonia ice, but which Irwin et al. (2001, Icarus, 149, 397-415) had pointed out should have produced a 2-micron absorption feature that was not observed in NIMS spectra (Brookes spectrum did not cover the 2-micron region). The VIMS spectra we looked at seemed to show evidence for a small 2-micron absorption as well as a large 3-micron absorption, suggesting that ammonia ice was indeed the main absorber (Sromovsky and Fry, 2009, Bull. Am. Aston. Soc. 41, 1009). However, as we applied the new inversion algorithm to more spectral observations, we found that ammonia ice provided a relatively poor fit to the brighter cloud features, and that NH_4SH provided a much better fit. Better still, we found that a mix of NH_4SH and NH_3 provided a better fit than either substance alone. This was also found when we reanalyzed the Brooke 3-micron spectrum (which has a much higher spectral resolution than the VIMS spectrum). Given that current models of ammonia absorption provide much more absorption in the 3-micron region than was present in the HITRAN96 model used by Brooke et al., it is not too surprising that our results are somewhat different. Fig. 2 displays a spectral fit using both NH_4SH and NH_3 absorbers.

The work on the development of a combination model of ammonia absorption and the application of that model to the high-resolution 3-micron ISO spectrum of Jupiter comprises the content of the first paper in progress listed in the publications section (Publication [1]). The best model seems to have ammonia and NH_4SH at nearly the same pressure level, suggesting that there might be two separate particle populations at the same level, or that ammonia may be appearing as a coating on the less volatile NH_4SH particles.
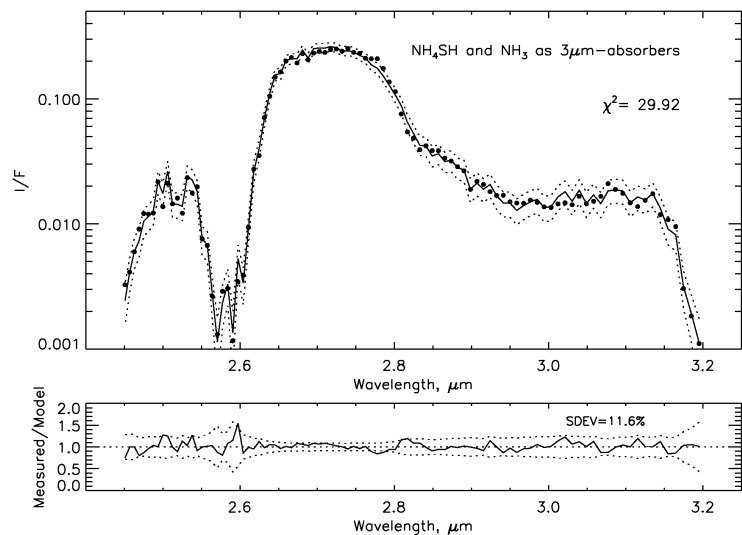
Figure 2. Spectral model fit to ISO spectrum of Jupiter. black dots show the model spectral points and the solid line is the ISO spectrum convolved to the same resolution as our absorption

4

In the second paper (Publication [2]), we applied the inversion technique to VIMS spectra at low and intermediate phase angles, providing spatially resolved results in regions of high (EZ) and much lower (NEB) cloudiness (the ISO spectrum had a large FOV that covered about a third of the Jovian disk). It is easier to see the need for a 3-micron absorber when the spectrum is fit with conservative clouds without a local absorber (Fig. 3, top panel).
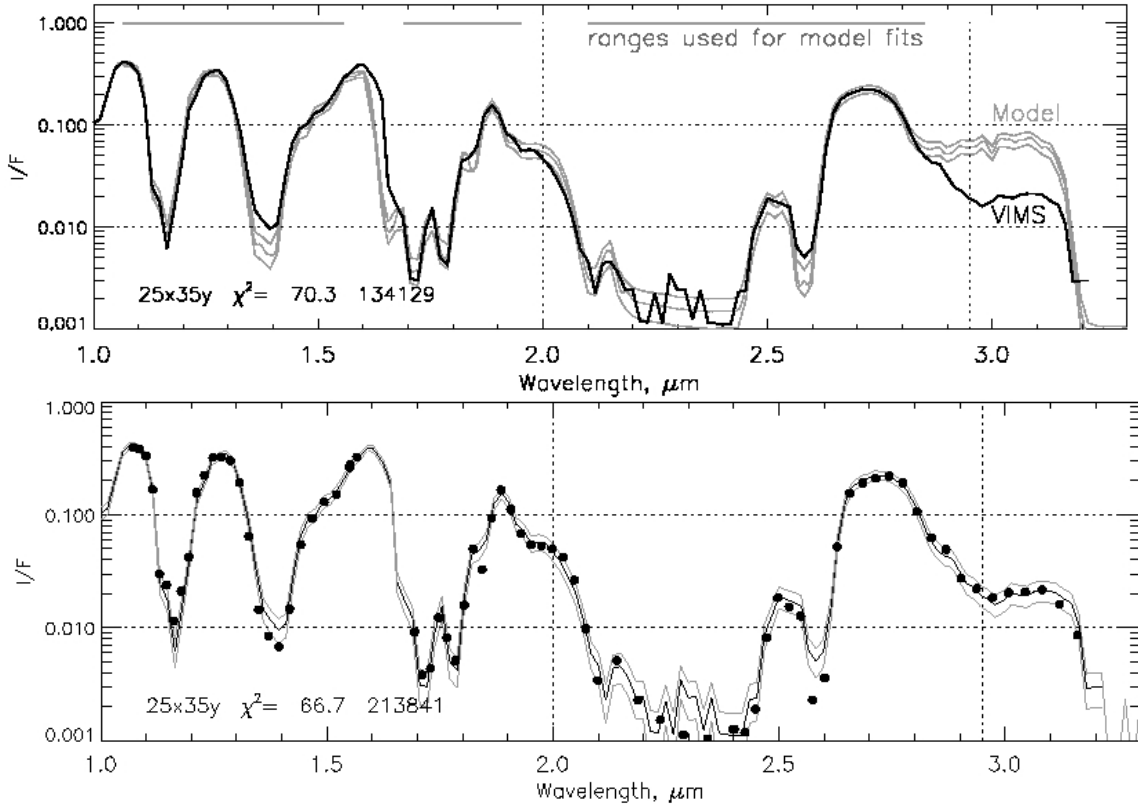
Figure 3. Top panel: here the fit is only constrained in the regions without expected absorption (denoted by gray bars). The gap near 1.6 bars is where the VIMS instrument response distorted by a joint between order sorting filters. The lower panel shows a model fit in which NH₄SH and NH₃ absorbers are both present in the model. Here the model points are shown as small filled circles.

We also tried to make use of a technique we planned to apply to the New Horizons LEISA observations, namely the use of spatial modulations at wavelengths of different penetration depths, to infer the pressure at which the spatial variations are taking place. This technique has the nice feature of ideally depending only on the ratio of modulations, not their absolute value, and also independent of the aerosol attenuation above the modulating layer, provided the attenuation is the same at the two wavelengths that are being ratioed. However, a complication in applying this to NICMOS imaging observations is that the two spectral bands of most value are the F204M filter and the F187N filter. Since the F204M filter contains the 2-micron region where ammonia can absorb, if most of the 3-micron absorption is due to ammonia, then the pressure level of the clouds inferred from the modulation ratio will be distorted. On the other hand, if most of the 3-micron absorption is due to NH₄SH, then the overlying clouds will not distort the ratio and a different pressure level will be inferred for the modulating cloud

layer. The result in Fig. 4 is for a preliminary estimate of how much ammonia ice is present above the modulating cloud layer. Note that the bright equatorial zone does not strongly correlate with the distribution of cloud pressures. It is mainly in the region of the plumes and just down stream from the GRS (off the image near latitude -20) where the highest spatially heterogeneous clouds are observed.
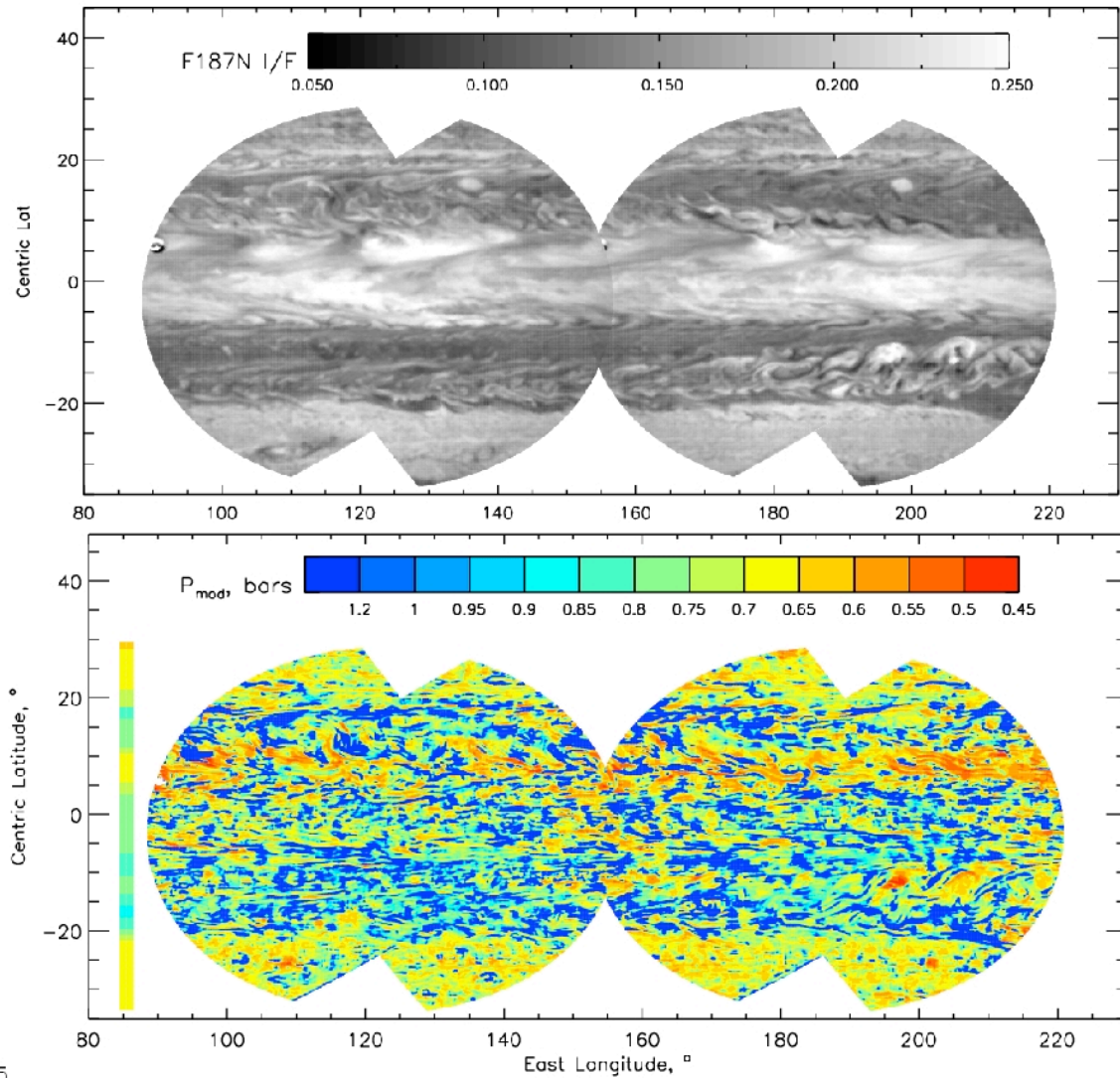
Figure 4. Top: F187N filtered image of Jupiter from HST. Bottom panel: pressure of spatially variable cloud layer inferred from spectral modulation ratio. The color bar for pressure is in bars.

We continued work on the problem of inversion of cloud structure from near-IR spectra (Task 3). The two papers that were in preparation the previous year (Publications [1] and [2]) were completed, submitted, revised, accepted (June 28, 2010), proofed, and published. A significant amount of work was involved in revising the ISO paper because one reviewer insisted on expanding the analysis of possible cloud compositions to include a wider range of chemical compounds than normally considered to be present in Jupiter's atmosphere. This work was useful in ruling out a larger range of possibilities. The best-fit alternative to NH_4SH turned out to be alcohol, which is not a plausible component of

Jupiter's clouds. Results from these papers were also presented at the 2010 DPS meeting in Pasadena in early October 2010.

Before beginning our detailed analysis of near-IR spectral observations, we became aware of recent advances in near-IR high resolution spectroscopic observations of methane absorption, raising the possibility that we might not be limited to band models in characterization of methane absorption in outer planet atmospheres. Band models have been a concern because they rely on data mostly outside the range of temperature, pressure, and path length that are encountered in giant planet atmospheres. The coverage problem is illustrated in Fig. 5.

The laboratory measurements providing the primary basis for the near-IR band models are by Strong et al. (1993, JQSRT 50, 363-429) and Sirha
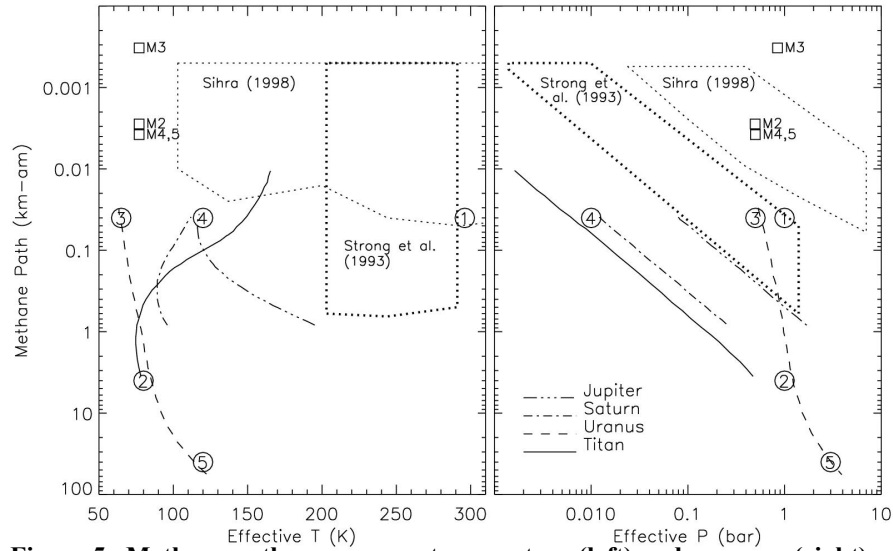
Figure 5. Methane path coverage vs temperature (left) and pressure (right).

(1998, PhD Thesis, Univ. of Oxford). Their coverage of the pressure-path and temperature-path regions are indicated by dotted and heavy dotted outlines respectively. The equivalent paths traversed in descending through outer planet atmospheres, as estimated by Karkoschka and Tomasko (2010, Icarus 205, 674-694), are seen to be generally outside the domains of laboratory measurements, even for Jupiter, which is the least deviant outer planet. The DISR measurements obtained during the Huygens probe descent into Titan's atmosphere, have helped to constrain band models for wavelengths less than 1.6 microns, but at a lower spectral resolution than the standard model calculations.

Line-by-line calculations, where lines are sufficiently well characterized with ground state energies and pressure broadening widths and containing sufficient numbers of weak lines, provide superior resolution as well as properly account for conditions on the outer planets. However, the line database up to HITRAN 2008 (Rothman et al. 2009, JQSRT 110, 533-572) has not been sufficiently complete to replace band models. New observations and new techniques, such as cavity ring down spectroscopy, have made great improvements in completeness, as illustrated in Fig. 6, which displays line strength and ground state energy levels for the HITRAN 2008 database in the top pair and a list we compiled from recent measurements in the bottom pair. Note the addition of many
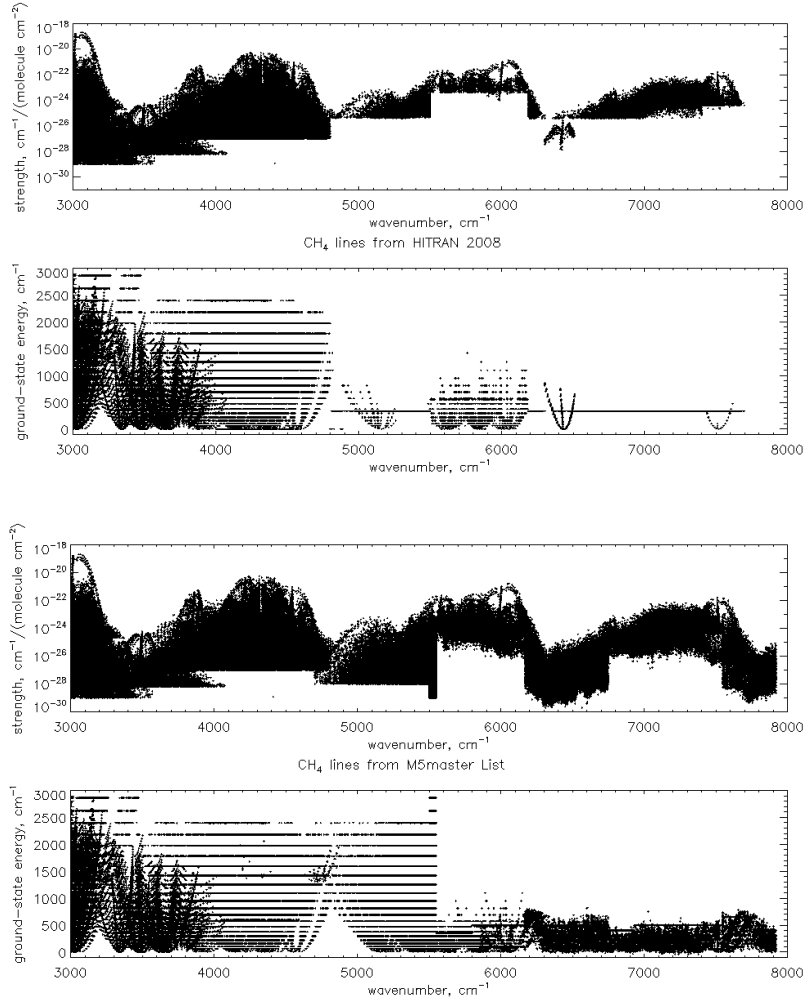
**Figure 6. Ground state energy and line strength coverage for methane.
Top panel is for HITRAN 2008 and bottom is for our extended line list.**

more low-strength lines, and the addition of ground state energy values for lines at wavenumbers beyond 5500 cm^{-1}. A comparison of line-by-line calculations using our new list, HITRAN 2008, and the two most recent band models of Irwin et al. (2006, Icarus 181, 309-319) and Karkoschka and Tomasko (2010) is displayed in Fig. 7 for an equivalent path found in the Jovian atmosphere. Our new LBL results (in red) are in generally excellent agreement with the band model results, except in regions between 5100 and 5500 cm-1, where the line databases lack information about CH_3D lines. This is a vast improvement over HITRAN 2008 (blue), for reasons apparent from Fig. 6. This indicates that the new line list is capable of accurate representations of methane absorption over a wider range of path conditions and at higher resolution than has been possible with current band models. A sample of comparisons at an extreme

8
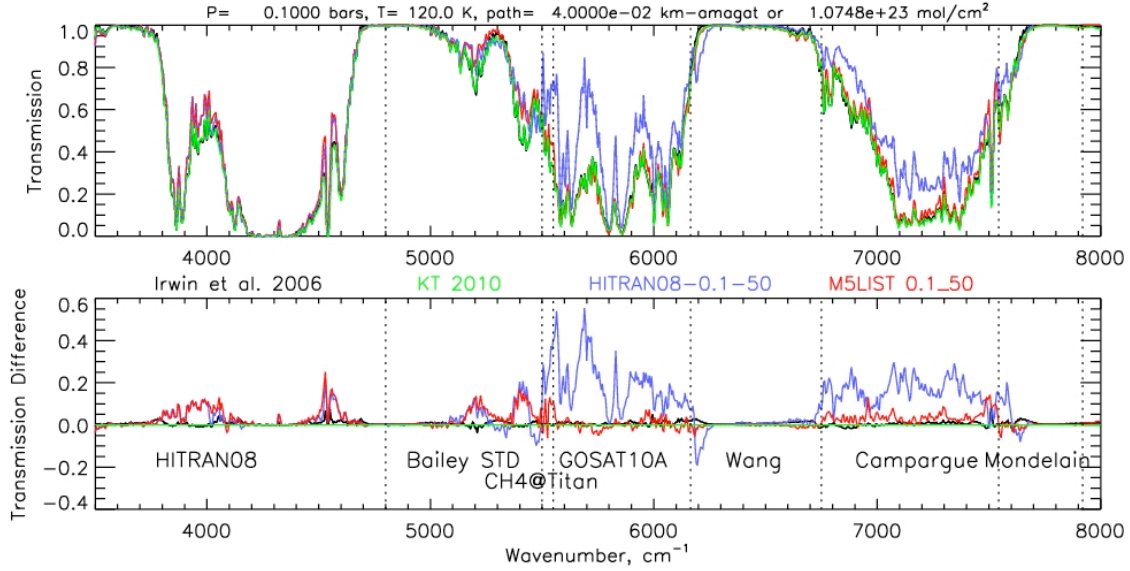
Figure 7. Comparison of different models of transmission through a path relevant to Jovian atmospheric conditions.

temperature is provided in the comparison (Fig. 8) with laboratory transmission measurements by McKellar (1989, Can. J. Phys. 67, 1027-1035) at 77 K. Our LBL results (shown in red) are far superior at this temperature to either of the two band models, both in the mean error and in the RMS deviation from the laboratory results. The LBL results are still lacking in several areas however, the region short of 1.28 microns lacks low strength lines and ground state energies, and there are regions

Figure 8. Comparison of new LBL model with lab measurements (see text).

where CH_3D is an important contributor, but where there is no line strength or energy information yet available. A paper on these results (Publication [3]) was published in 2010.

We also began preliminary analysis of CCD image data in combination with spectra (Task 5). We explored three constraints to be applied to cloud structure models, just from Cassini ISS observations of Jupiter: (1) center-to-limb variations, (2) spectral variations from bandpass filter to filter, (3) spatial modulation ratios in pairs of filters that have different sensitivity to gas absorption, but close enough together in wavelength to have the same sensitivity to aerosol contributions.   We extracted center-to-limb

9

variations for individual cloud features using a sequence of ISSNA images in which the feature drifts across the disk, but not too long to allow substantial feature evolution.
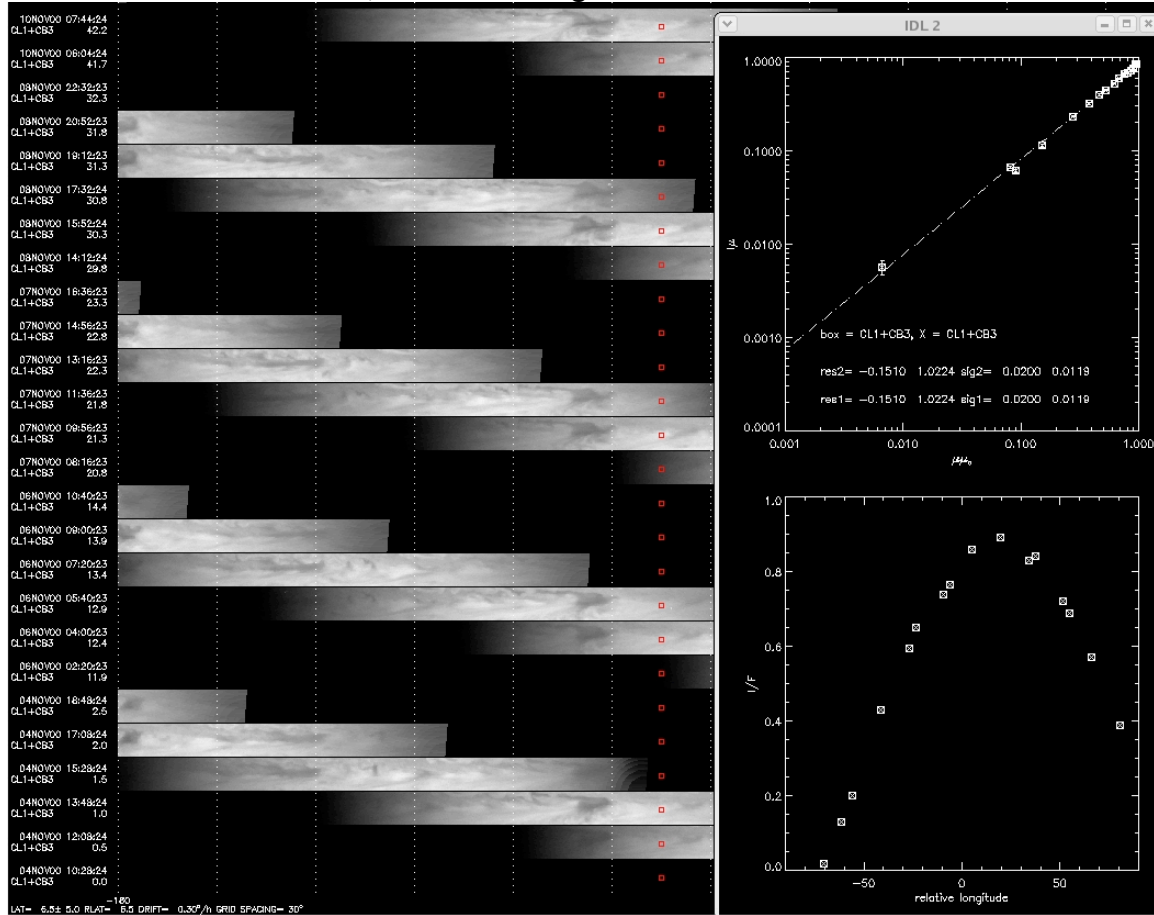
Figure 9. Left: VIMS images of Jupiter, remapped into narrow longitudinal strips, then shifted by relative wind drift to vertically align features in a chosen latitude bin (here centered at 7 deg N and covering 10 deg in latitude, displayed with time increasing upward. The chosen target points (red squares) are displayed in a Minnaert plot (upper right) and center-to-limb profile (lower right).

The target selections are made in a deeply penetrating filter (here CB3 (938 nm) was used), and corresponding target data from eight other filters are automatically extracted from corresponding latitude-longitude locations in those images. This results in a spectral and center-to-limb constraints as indicated in the following figures for a dark feature (left) and a bright feature (right). These are only two targets among many in just this bin, and there are many latitude bins as well, which should result in a bounty of individual feature data sets. We implemented the tools to ready for data extraction, but still had work to do to implement the fitting algorithm that would constrain the bandpass filter constraints.
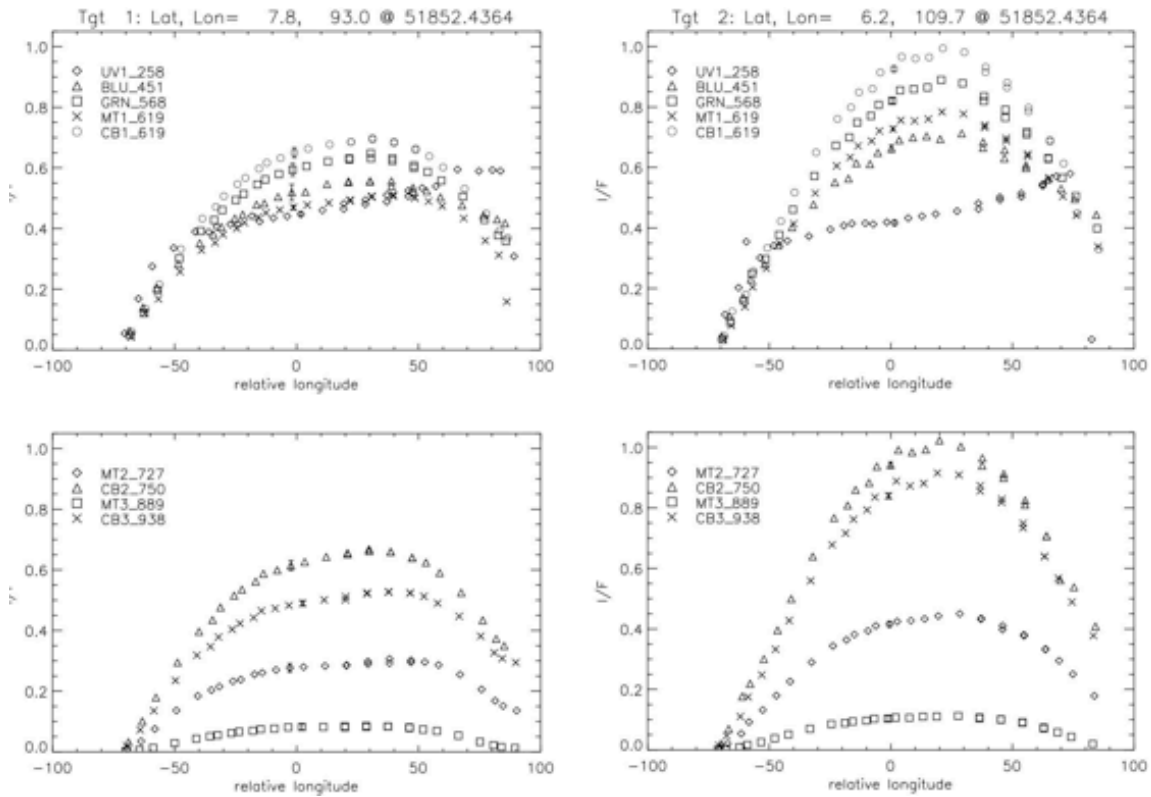
Figure 10 Center to limb profiles for bright (left) and dark (right) cloud targets selected as shown in Fig. 9.

Applying spatial modulation analysis to retrieve cloud pressures from the NICMOS data, yielded plausible pressure maps, with most clouds in the 0.7-1.2 bar range. However, the use of F204M and F187N filters for this purpose is somewhat suspect because of uncertain absorption by NH_4SH and/or NH_3 particles in the F204M filter band. To provide a cleaner spatial modulation result, we applied the technique to Cassini ISS images of Jupiter, using MT2 and CB2 filters initially. A formula to relate the ratio of spatial modulations in MT2 to those in CB2 was developed from model calculations. The started with a base model that fit Jupiter's geometric albedo spectrum. The effects of perturbations of the middle cloud optical depth at a range of pressures surrounding the best-fit pressure on the model I/F values for MT2 and CB2 then provided the needed relationship. However, the result of applying this empirical model result to the observed ratios resulted in unexpectedly high pressures, roughly twice the values expected from the near-IR analysis. A sample pair of remapped images and target boxes are shown in Fig. 11, along with the pressure inferred from the modulation ratio. Here there are two remapped images in CB2 (750 nm) and MT2 (727 nm) filters displayed at the bottom. Two small boxes show the regions from which I/F values are extracted. The plot at the upper right shows a plot of MT2 vs CB2, and the linear fit that determines the slope, from which the pressure modulation formula yields a pressure of 2.45 bars. The upper left plot shows a scan vs latitude through the target region (bounded by dotted lines) and adjacent to that plot is a blowup of the target regions for each filter.

11

A major stumbling block in our planned analysis of both Cassini ISS and New Horizons LEISA spectral images is that this visible-near IR inconsistency in modulation pressure inferences needs to be understood.
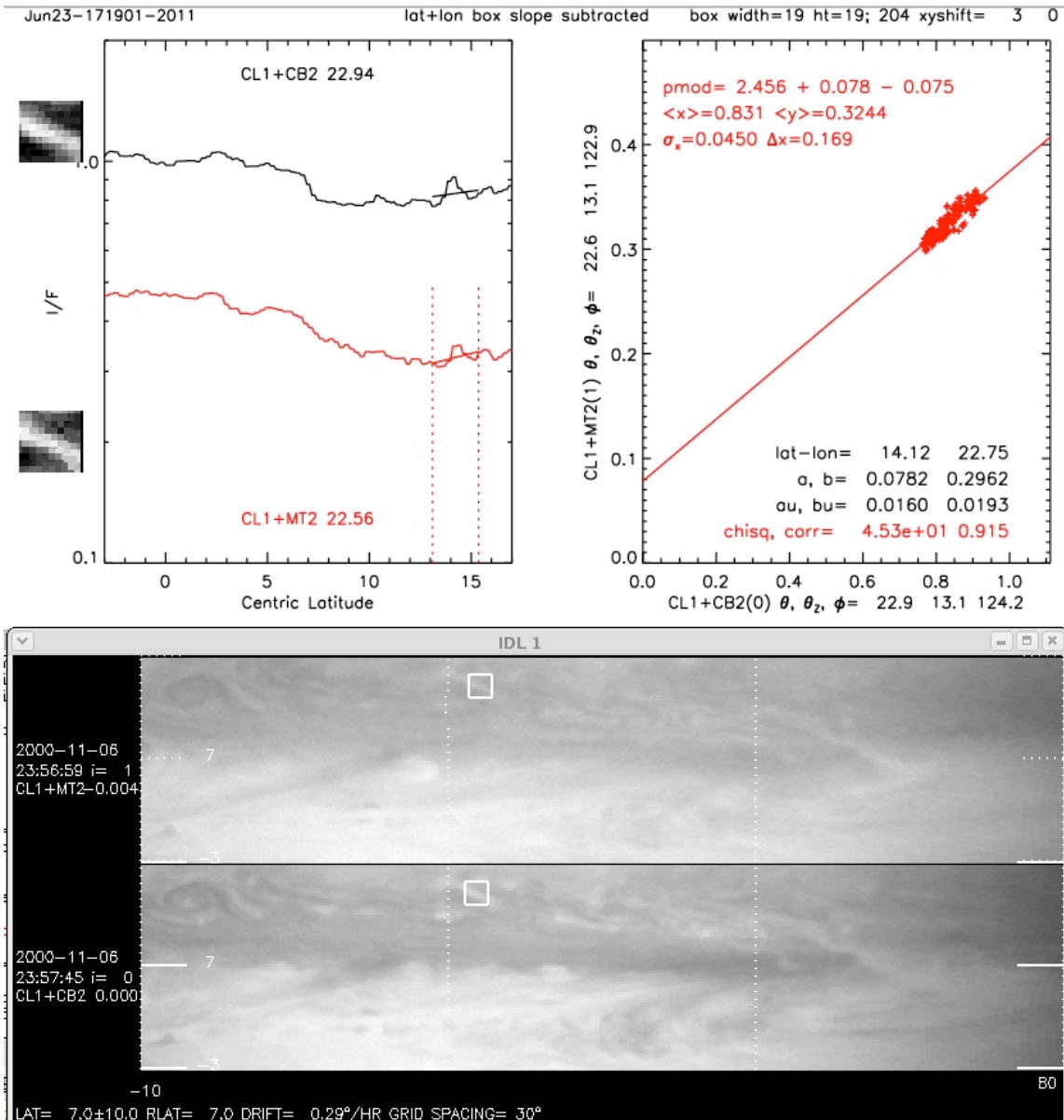
Figure 11. Application of spatial modulation to infer cloud pressure (see text).

PROGRESS DURING YEAR 3

An abstract on the comparison of line-by-line and band models near-IR methane absorption was presented at the joint EPSC-DPS meeting in Nantes in early October 2011 (Publication [8]). We also completed and submitted the Icarus paper on the same topic, then withdrew it and resubmitted an improved version with inputs from additional authors who were brought on board in recognition of their primary responsible for the

laboratory measurements and theoretical modeling of methane absorption line properties. After reviews were received, the paper was slightly revised, resubmitted, accepted on 9 December 2011, and subsequently published (Publication [3]). This was the main accomplishment of Year 3, as progress on other tasks was greatly slowed by resource conflicts with other projects. To allow time to complete the remaining tasks we asked for and received a no-cost extension until 30 April 2013.

Analysis of CCD image data in combination with spectra (Task 5) remained in its initial stages, remaining at essentially the same state as described in last year's progress report.

A paper we had hoped to write on the analysis of NICMOS observations of Jupiter also did not progress much, primarily because of uncertainties in how to handle potential absorption by NH_4SH and/or NH_3 particles in the F204M filter band, complicating the spatial modulation analysis, which is only simple if the aerosol properties can be assumed the same for both filter bands. As noted in last year's report, we also applied the spatial modulation technique to Cassini ISS images of Jupiter, using MT2 and CB2 filters initially. However, the result of applying this empirical model result to the observed ratios resulted in unexpectedly high pressures, roughly twice the values expected from the near-IR analysis. This visible-near IR inconsistency in modulation pressure inferences needs to be understood, and we hoped that the New Horizons LEISA observations might provide a good data set for reaching that understanding because it provides near-IR wavelengths that provide useful vertical sensitivity ranges but avoid potential particulate absorption features.

However, our progress also was slow in making needed corrections to New Horizons LEISA spectral imaging observations that are needed to obtain calibrated spectra of discrete features. The image in Fig. 12 is from an acquisition sequence of 1354 256x256 multi-wavelength images, each with an exposure time of 0.349 sec, for a total observation duration of 472 sec (7.87 min, or 4.76 deg of longitude). The image is recorded in two spatial dimensions, with a wedge filter that makes one dimension also vary with wavelength. A full spectrum for the target region thus requires spatial scanning in the direction in which wavelength varies, taking image frames at each scan step. A monochromatic image can then be formed by assembling from top to bottom, line by line, the same wavelength row from each successive frame of the observation. The consequences of this are that each row of a monochromatic image has an effective acquisition time different from all other rows, and that different monochromatic images have different start times. This means that a specific cloud target can, and generally will, appear at different image locations at different wavelengths. This would be true even if the camera pointing did not vary during the image scan, which it does, and even if the cloud target stayed at the same latitude and longitude, which it does not. The waviness seen at the edge of the image is a result of variations of camera axis pointing during a scan of the planet.
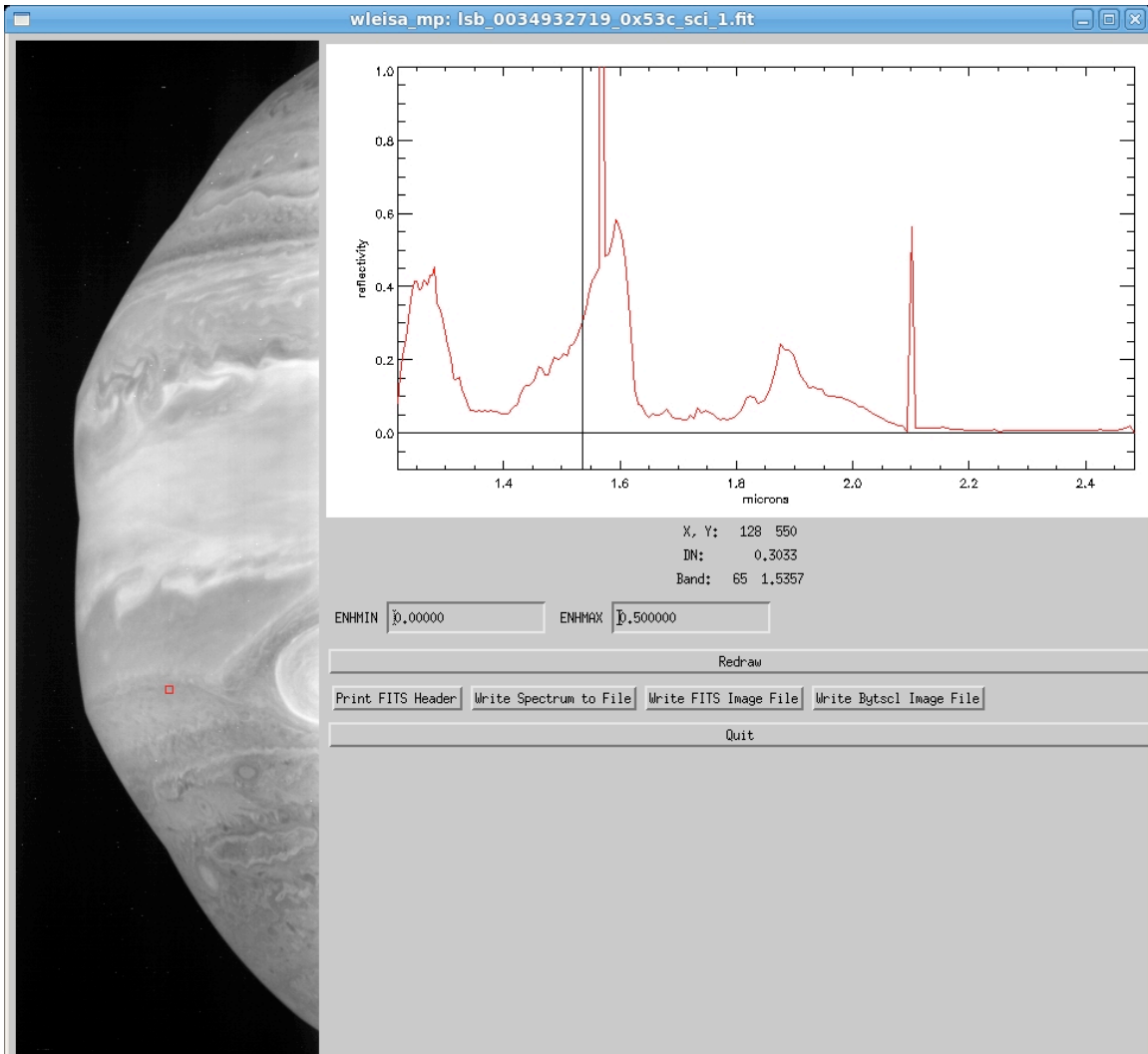
Figure 12. Sample use of our LEISA viewer to display images and target spectra.

The calibrated PDS observation cubes have all the information necessary to determine a given pixel's coordinates in space and time. For every pixel of the multi-wavelength 256x256 pixel frame, there is a vector for that pixel relative to the optic axis of the instrument. In addition, for each frame of the observation, there is the ephemeris time and pointing information for optic axis of the instrument. These data allow us to account for planetary rotation when extracting spectra from the planet, so that a spectrum will have a fixed latitude and longitude on the planet, and also to remove the waviness seen in the sample monochromatic image.

PROGRESS DURING YEAR 4:

Work on processing eleven VIMS data sets to produce calibrated cubes with navigation backplanes was carried out in support of a paper on Jupiter's total emitted power (Publication [4], with Liming Li, prime author).

Our progress in making needed corrections to New Horizons LEISA spectral imaging observations, that are needed to obtain calibrated spectra of discrete features, was slowed in part because we were not able to apply sufficient effort to the task due to resource conflicts with other projects and with proposal and proposal review efforts. However, this year we did make considerable progress and reached a point at which corrected image cubes were created. This has been a complicated correction.

The first step was to extract and process pointing information so that observations can be remapped to a latitude-longitude grid for each wavelength, with backplanes of time and viewing geometry. Since the wavelength varies slightly across a line in the raw image plane, we also had to interpolate in wavelength, which is in the y-direction in the raw image plane. We produced prototype image cubes with dimensions of latitude (0.25 degree spacing), longitude (0.25 degree spacing), and wavelength (5 nm spacing). This remapping takes out the major factor that causes cloud features to appear at different image locations in different wavelengths. An additional refinement in the remapping would be to compensate for motion of features, due to Jupiter's zonal wind field. For individual dataset cubes this compensation is probably not necessary, though it would be required for any mosaicking of multiple cubes. In Fi.g 13, we show two bands of a remapped cube as a red/green image. In the blowup of the equatorial region, seen in the lower left window, there are dark features with longitudinal extents of around 0.5 degrees. With a per-image exposure time of 0.314 seconds, there is approximately 0.5 degrees of rotation of the planet between the acquisition of the lines of different wavelength. If the navigation and remapping of image lines widely separated in wavelength were not accurate, dark (or bright) features of that size would not remain coherent.

There remained some serious dataset anomalies to be dealt with. One particularly vexing problem was in the radiometric calibration. The calibrated PDS data are claimed to be inappropriate units. Whereas the relevant project document (New Horizons SOC to Instrument Pipeline ICD) states that the units are radiance (with units $W/cm^2/sr$, which is not a spectral radiance because it lacks a spectral divisor), the units actually appear to be spectral photon radiance (photons/sec/micron/sr). The instrument team has not been able (or able to find time) to confirm this. There are also some residual raw image bias or scattered light issues. Bias in the raw images manifests itself as vertical streaks in the processed monochromatic images. Where scans begin and end off the planet, blank bias images (that are subtracted from each raw image) can mostly rectify the problem. However, when the planet fills the entire scan (as is the case for several of the datasets), this correction cannot be applied.

In preparation for carrying out the proposed principal component analysis, we acquired the IDL-based software called ENVI, which is specifically designed to facilitate the analysis of hyperspectral data sets, like the one generated by LEISA. This has been installed, and utilities have been written to generate ENVI-compatible image headers, and the datasets can now be read by and manipulate by ENVI. We can thus use ENVI's PCA and classification tools to explore the datasets. Fig. 13 shows an ENVI display of a LEISA cube with magnified section, along with an extracted spectrum.
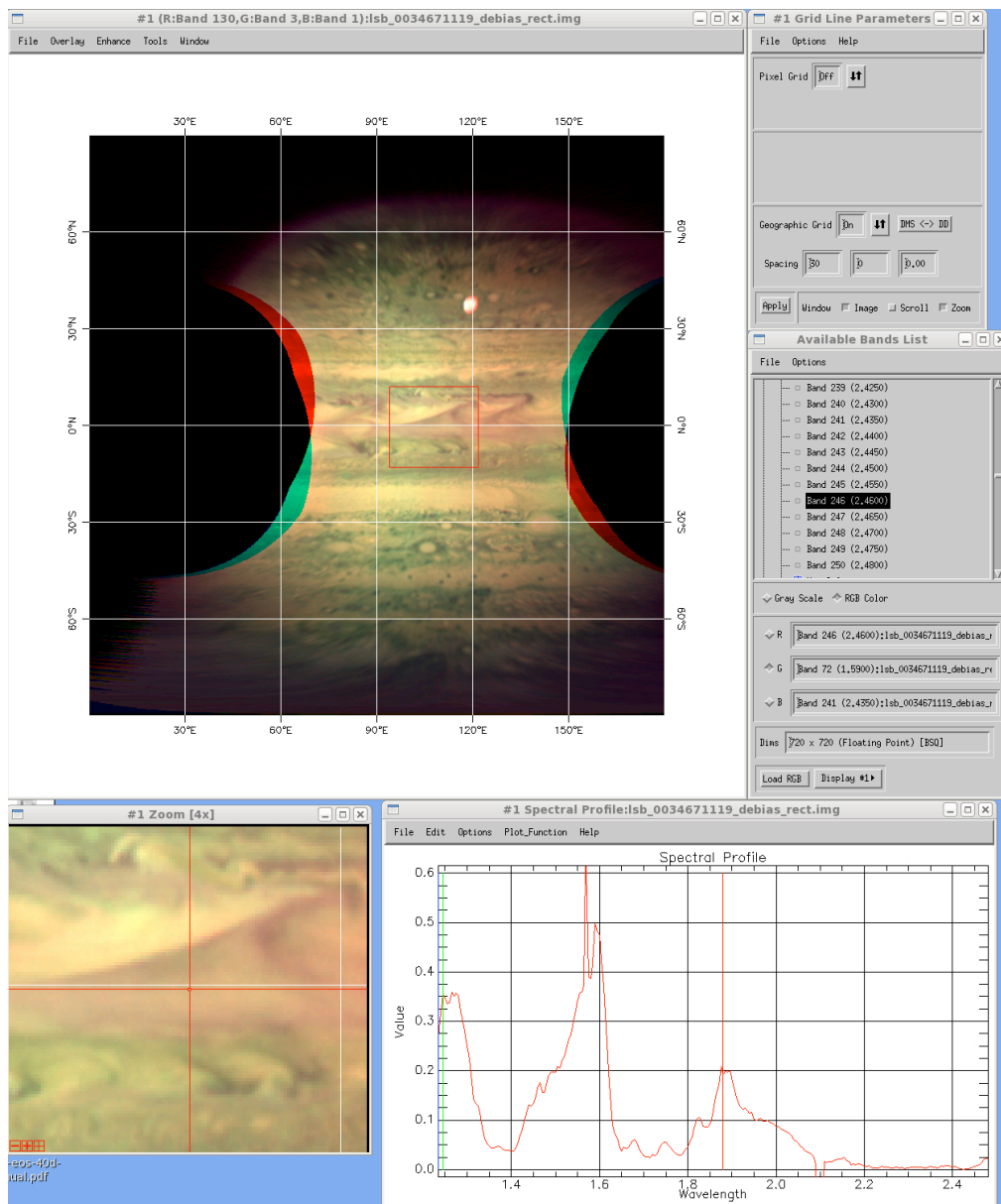
Figure 13. ENVI display comparing corrected and remapped LEISA images at two wavelengths to verify geometric alignment of wavelengths acquired at different times.

We also began to compare LEISA observations with NICMOS and VIMS observations of Jupiter, to provide a sanity check on radiometric calibration and offset (or low light level) issues, as well as to begin the process of characterization of temporal changes between Cassini (2000) and New Horizon (2007) epochs (task 4). Images from all three data sets are shown in Fig. 14. Although a precise comparison is prohibited by time differences between the data sets, we find general agreement on the I/F calibration that we have assumed (based on units of photon radiance) but, as illustrated in Fig. 15, we find significant discrepancies in the regions of low I/F.
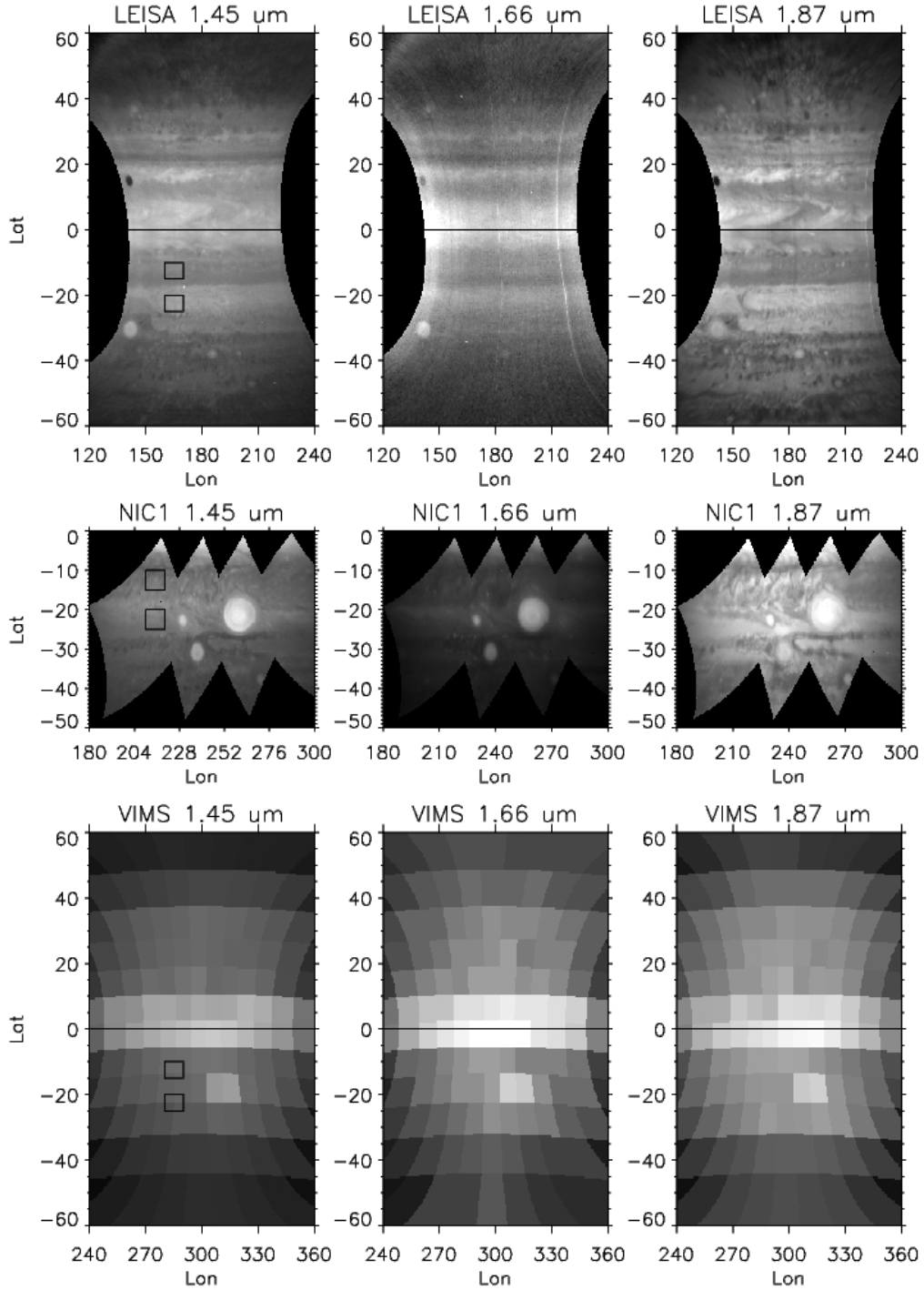
Figure 14. Comparisons of remapped images of Jupiter from LEISA (Feb 2007), HST NICMOS (May 2008) and VIMS (December 2000). Spectral comparisons in Fig. 15 were made for SEB (10S-15S) and STZ (20S-25S) to avoid regions with significant temporal changes. Spectra in Fig. 15 were extracted from regions marked by black squares .

In Fig. 14, black to white corresponds to the I/F range of 0-0.18 for the 1.45-micron images, 0-0.05 for the 1.66-micron images, and 0-0.25 for the 1.87-micron images.
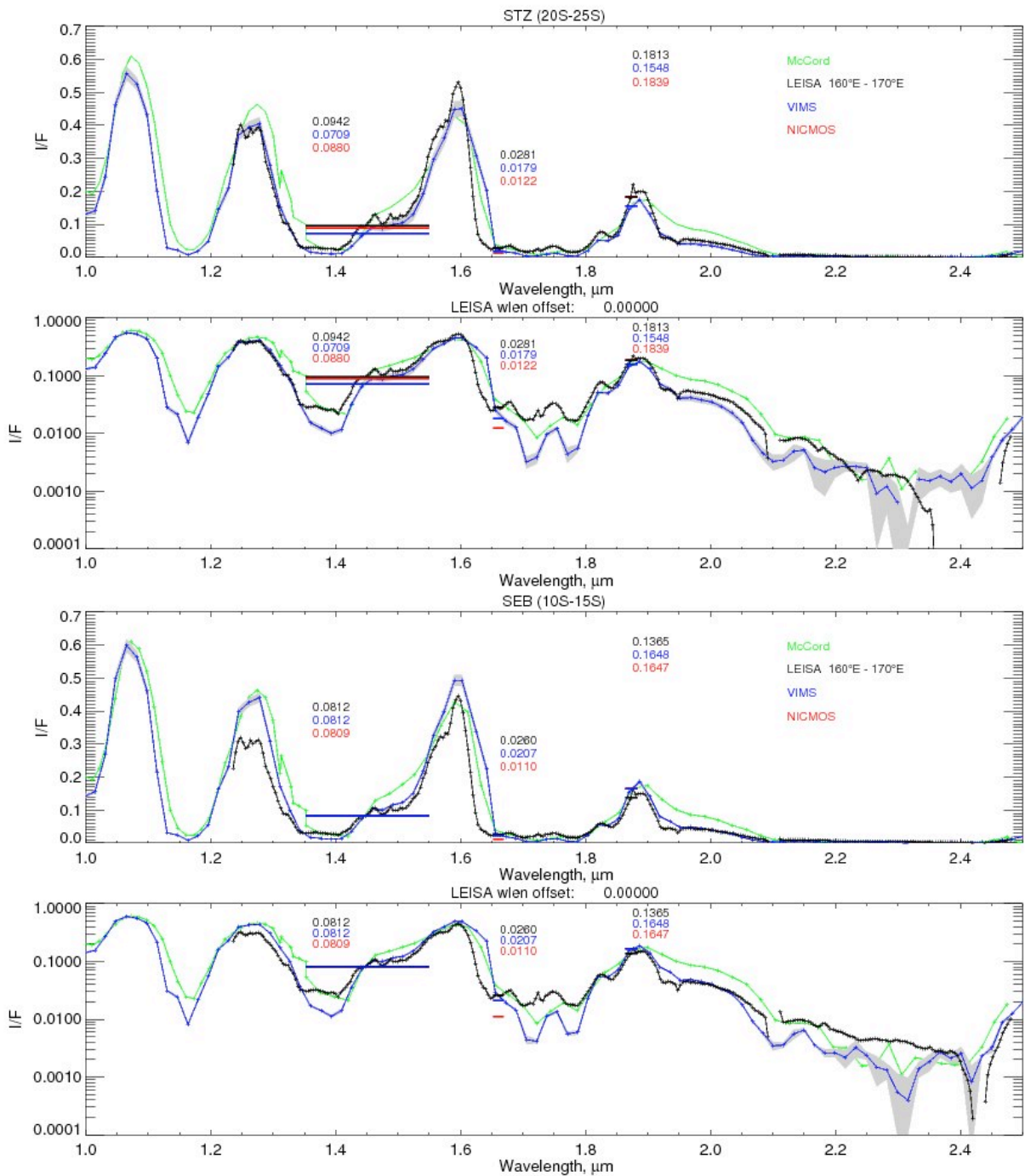
Figure 15. Comparison of spectra from LEISA (lines with points) and VIMS (shaded, blue), NICMOS (red) , and McCord et al. (green). Specific locations from which spectra are obtained are indicated in Fig. 14. The comparisons should be ignored in the 1.6-1.68 micron region where VIMS artifacts are present.

 The plots in Fig. 15 also illustrate a potential problem with low-I/F regions of the spectrum, although this might be due to temporal changes in high altitude haze amounts.

These are the first detailed comparisons we know of between LEISA and VIMS atmospheric spectra.
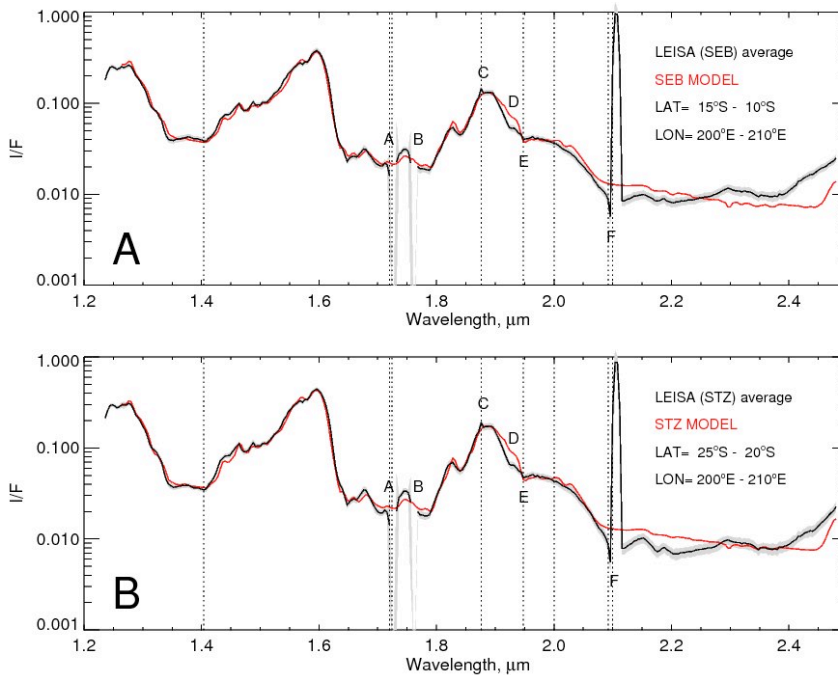
Figure 16. Comparison between LEISA spectrum (red) and model spectrum (black). This validates the LEISA wavelength calibration and demonstrates the compatibility of LEISA observations and radiative transfer modeling of Jupiter's spectrum.

For the comparison between LEISA observations and model calculations provided in Fig. 16, we used a 3-layer model aerosol model, characterized by pressure, particle size, optical depth and effective pressure. The spectral details are generally well matched by the model.

I/F value disagreements in Fig. 15 between LEISA and VIMS spectra in the strongly absorbing regions might very well be due to temporal variations in haze optical depth. However, the NICMOS 1.66-micron image from 2008 is quite a bit darker (in Fig. 14) than either VIMS or LEISA, suggesting that they may both be suffering from a low light level problem. Further analysis of such comparisons may be needed to settle this issue. A more meaningful comparison will be possible once LEISA spectral data cubes are integrated over appropriate bands with appropriate weighting to simulate the spectral weighting of the NICMOS band-pass filter images. We asked for and received a second no-cost extension.

RESULTS FROM FINAL YEAR OF EFFORT

Software upgrades have resulted in a unified retrieval code that can handle VIMS, NIMS, and LEISA observations of Jupiter. The most challenging has been the LEISA observations because of all the corrections required and because the PDS data sets are not correctly calibrated and the instrument teams have not been able to provide much help in correcting the calibration. We finally obtained what we believed to be the correct radiometric calibration for the data sets we plan to use and started fitting spectra of cloud

features that have been identified as relatively more absorbing at 2 microns than typical clouds, a likely reason being that they are composed mainly of NH_3 ice. A sample of image of selected features is provided in Fig. 17.
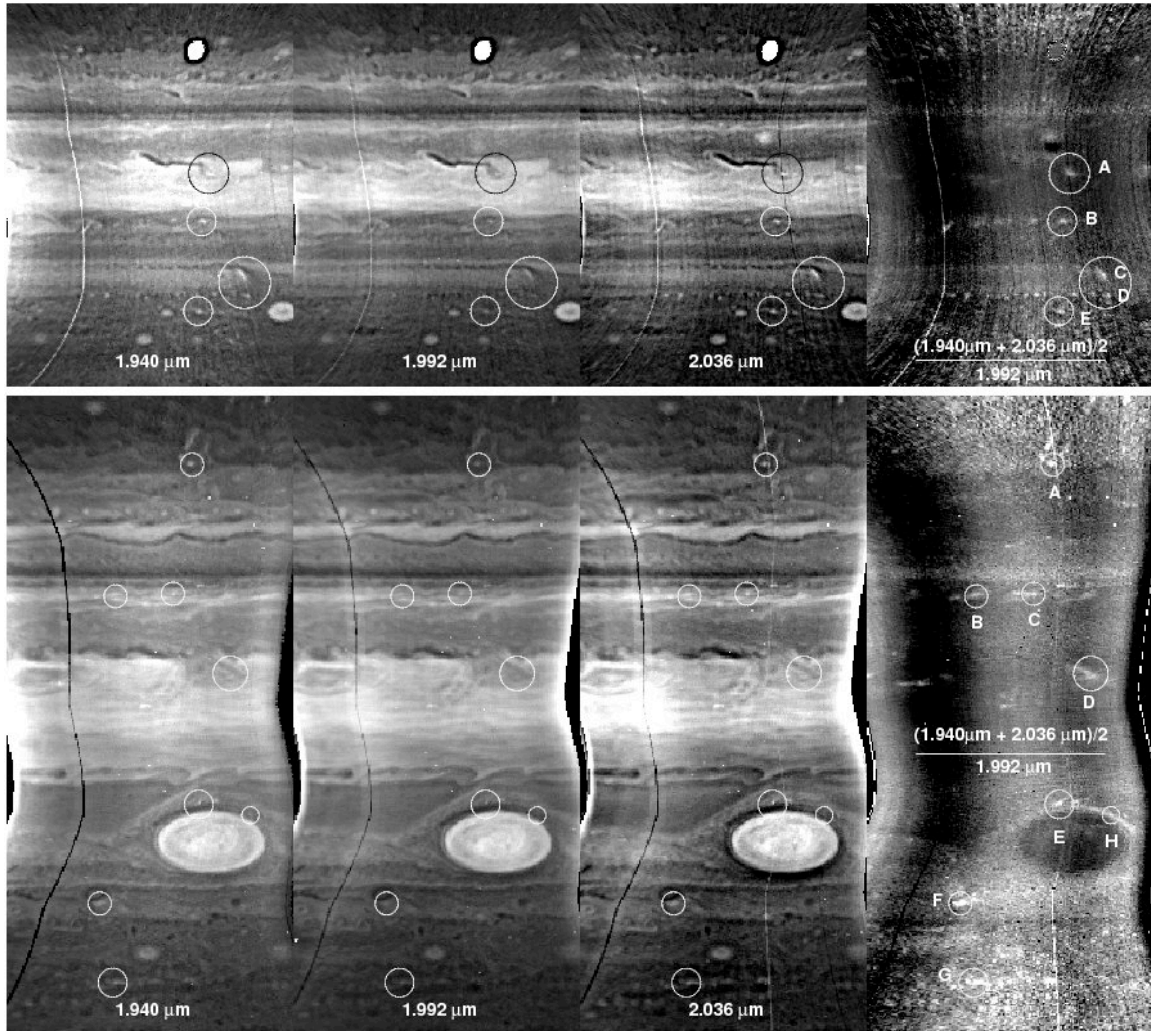
Figure 17. LEISA images of Jupiter at 1.992 microns, near the 2-micron NH_3 absorption feature, and at both sides of it (at 1.94 microns and 2.036 microns), and the ratio of the absorbing I/F to the mean I/F of the non-absorbing adjacent wavelengths (far right panel). Circled regions help to locate the sample features that exhibit absorption typical of pure NH_3 ice. Observations are from August 2008.

A spectrum from feature C in the upper right panel of Fig. 17. is displayed in the Fig. 18 in comparison with a model fit using NH_3 as the cloud material and a spectrum in which NH_3 is replaced by a material with the same real index but without NH_3 absorption features. This clearly shows that pure NH_3 ice is a good fit to the dip at two microns.
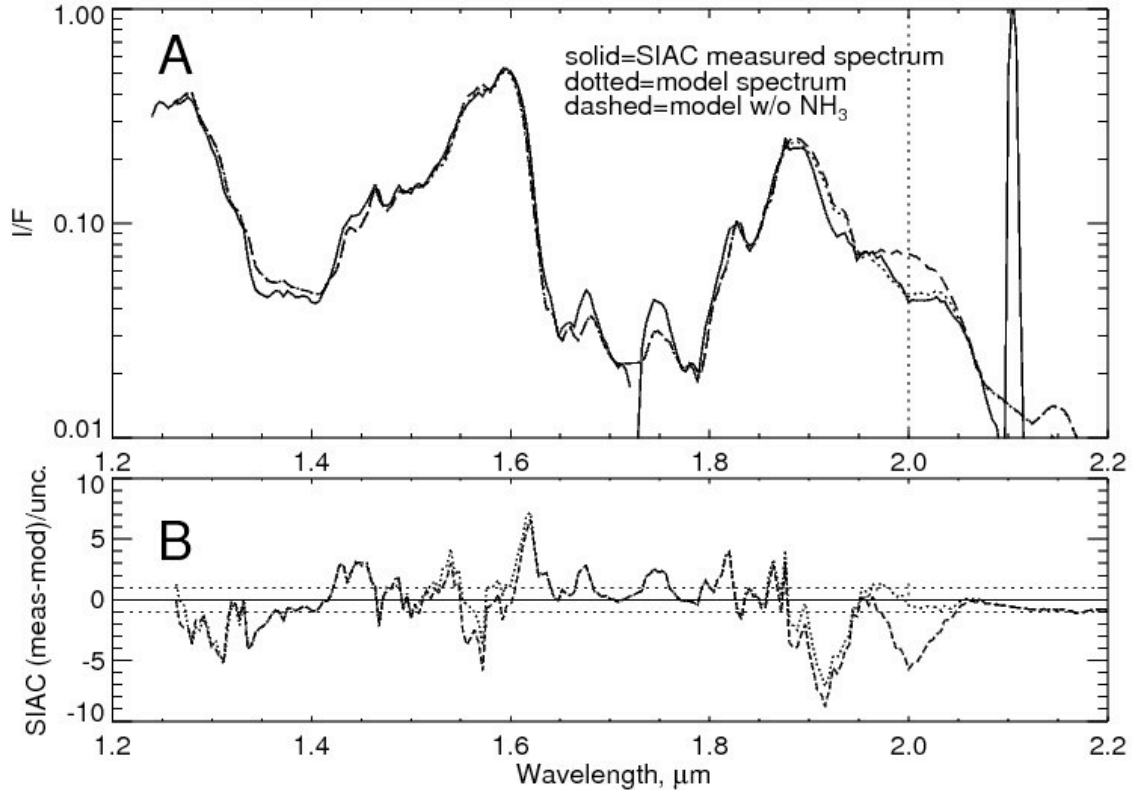
Figure 18. Comparison of observed (solid) SIAC spectrum with models containing NH₃ ice (dotted) and containing an absorption free substance without NH3 absorption features (dashed).

We have also begun fitting NIMS spectra that simultaneously provide spectra near 3 microns and 2 microns, which are both regions of NH_3 absorption. This has been a more difficult task because the NIMS noise level is so large that considerable averaging is needed to retrieve the spectral features in both 3-micron and 2-micron spectral regions. We focused on the main SIAC feature first identified by Baines et al. (2002). To locate regions that have both 2-micron and 3-micron (actually 2.965-micron) absorption features we filtered the data in various ways indicated in Fig. 19. The spectra shown are indicated for several different conditions on the spectral signature ratio. The spectrum in A is for the strongest absorption at 2.74 microns, which is the brightest green region in (a) and the brightest red region in (b) and (c). This is a region that should be the prototypical SIAC region. In fact we do find NH_3-like signatures near 2.0 microns and 2.965 microns, but slightly displaced from their expected positions towards longer wavelengths, which might be a result of composite particle structure. The spectrum in B is mainly from the regions near the edge of the SIAC feature, but includes all of the yellow regions shown in (d), where significant absorption is present at both 2.0 and 2.965 microns. This selection does indeed have absorption exactly at the expected wavelengths and exhibits the cleanest spectral signature of NH_3 ice, even though it is brighter at 2.74 microns than the region sampled by spectrum A. The spectrum in C samples the SIAC at intermediate values of the 1.61/1.274 micron ratio and provides only a hint of the NH_3 ice signature. This is a strange result, i.e. the center or peak absorption region of the region has slightly displaced NH_3 absorption peaks, the edge having well matched absorption

spikes, but in between hardly any evidence of NH$_3$ at all. It is hard to imagine what cloud development or particle growth/evaporation scenario could explain this difference. The spectrum in D is the average over the entire imaging area. The complete absence of the NH$_3$ absorption spikes in this average shows what a tiny fraction of the region actually contains these spikes.
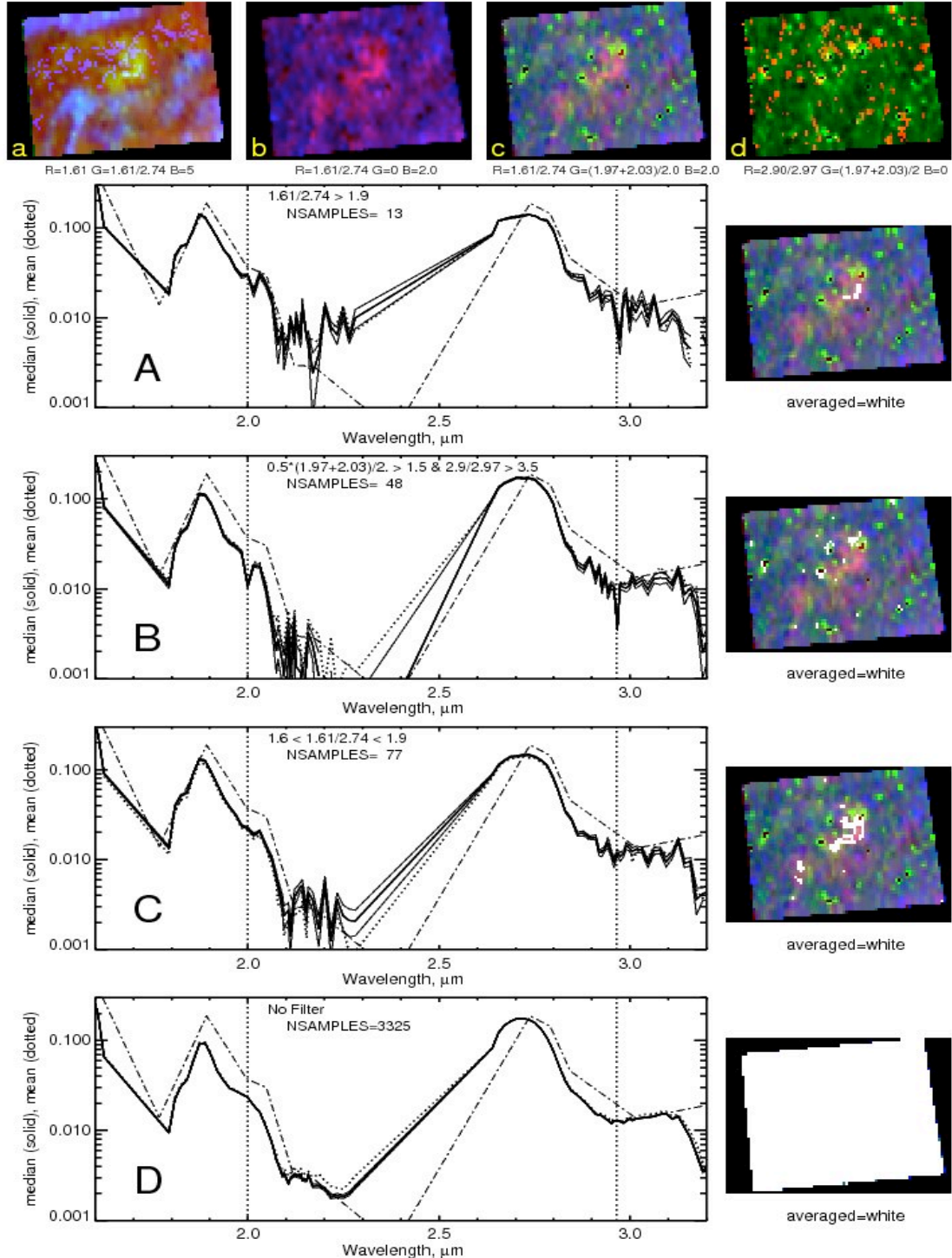
Figure 19. NIMS images and spectra in the region containing a major SIAC feature (see text).

We have found it difficult to create models that reproduce the spectral features in the NIMS spectra, from region B in particular. A layer of NH_3 ice particles that can produce a sharp 2-micron absorption feature seems to require large particles (~10 microns in radius), but when vertically distributed as required to match methane absorption bands, the gas absorptions mixed in with the aerosols attenuates the absorption feature. Also, the sharp absorption features at 2.965 microns, when averaged over the NIMS line-spread function, actually disappears for the large particles. If we use only small particles (~2 microns) the 2.965-micron structure is easy to reproduce (though it is somewhat broader than the NIMS measurement), but the 2-micron feature disappears. We have had some success by combining an optically thin layer of small NH_3-coated particles over a layer of larger particles, which can produce features at both 2 and 2.965 microns, but so far have not been able to closely match the depth and width of the 2-micron feature (in NIMS measurements). The sharpness of the NIMS 2-micron feature is surprising, considering that the NIMS FWHM (25 nm) is broader than the LEISA's (9-10 nm), while LEISA spectra show a broader 2-micron feature than is apparent in the NIMS spectra.

These preliminary results have been put into a draft paper concerning the quantitative analysis of "fresh" ammonia ice (Publication [5]). However, this analysis and resulting publication could not be completed with the remaining funds in the subject grant. It will be completed under support of a subsequent grant from the Planetary Atmospheres program.